GEOPHYSICAL AND GEOCHEMICAL OBSERVATIONS ON MUD VOLCANOES FROM PÂCLELE MICI, ROMANIA

FLORINA CHITEA[1,2], HORIA MITROFAN[1], ILIAS FIKOS[3], IRINA MARILENA STANCIU[4], CONSTANTIN DIACOPOLOS[1], RĂSVAN STOCHICI[1]

[1] *Institute of Geodynamics of the Romanian Academy, Bucharest, Romania*
[2] *Faculty of Geology and Geophysics, University of Bucharest, Romania*
[3] *Exploration Geophysics Laboratory, Aristotle University of Thessaloniki, Greece*
[4] *National Research and Development Institute for Marine Geology and Geo-ecology – GeoEcoMar, Bucharest, Romania*

Four main locations with clusters of active and dormant mud volcanoes occur along the axis of the Berca-Arbănași anticline structure. The active vents are releasing methane-rich gas and ejecta mixture of salty water and fine-grained material. Evaluation of the chemical composition of the ejecta material revealed several differences among the four main locations, the external sources (Fierbători and Beciu) presenting a more mineralized ejected liquid. The present study is focused on the near-surface internal structure of the Pâclele Mici mud volcanoes and its ejected fluids chemical composition (gas and saline, NaCl-type groundwater). Pâclele Mici mud volcanoes site was geophysically investigated by means of Electrical Resistivity and Spontaneous Polarization methods. The results were correlated with on-site observations of active mud volcanoes as well with older database. A lateral spread of the upraised fluid was noticed at shallow depths (<10 m), suggesting changes in sediments permeability or a significant decrease of the muddy material energy at shallow depth. The Spontaneous Polarization (SP) method proved to be a reliable tool for tracing the mud volcanoes feeder channels that branch from the main deep conduit.

Key words: electrical resistivity tomography, mud volcanoes, anticline structure of Berca-Arbănași, Buzău County, Romania.

1. INTRODUCTION

Mud Volcanoes are structures usually created by a very long-term process in which, due to natural Earth forces, large quantities of a mixture of gas, water and fine-grained sediments are expelled at the Earth surface, taking in time different external morphological shapes. The gaseous emissions accompanying the ejected muddy material are, for most of the sources, methane rich (also petroleum products being sometimes conveyed by the main geo-extruded material), while fewer sources present emissions with nitrogen as the dominant gas. Detailed studies on mud volcanoes (Barber *et al.*, 1986; Ivanov *et al.*, 1992; Dimitrov, L.I., 2002; Mazzini *et al.*, 2009) emphasized mud volcanism as a phenomena caused by a wide range of geological, hydrogeological and tectonic factors.

There are several models for the internal structures of mud volcanoes systems, the basic structural model of a kilometer-scale consisting in a source domain, a feeder channel and the mud edifice formed at the Earth surface. Overall, it seems there are not enough data to understand all the processes that occur in a mud volcano system and the corresponding triggering mechanism. Most studies used seismic reflection method to gather an image of the mud volcanoes system deep structure (mainly for marine mud volcanoes structures), but often resulted in a poor quality images, generally due to the technique difficulties in such environment (Hovland, Judd, 1988, in Judd and Hovland, 1992; Perez-Garcia *et al.*, 2011). Therefore, the geometry of the deep part of a mud volcano structure remains poorly documented.

Geoelectrical methods have been recently applied for getting a detailed view of the upper part of the mud volcanoes systems (Sung *et al.*, 2010; Zeyen *et al.*, 2011; Rainone *et al.*, 2012; Chitea, 2016; Diacopolos, Stochici, 2016). Structural mud volcano models with very shallow mud accumulation “chamber” or "shallow buried reservoirs" (usually at less than 35 m deep) were interpreted in few locations based on electrical resistivity tomography (ERT) measurements (Zeyen *et al.*, 2011) and seismics (Accaino *et al.*, 2007; Rainone *et al.*, 2012), while in other studies the specific development of the mud volcano structures did not contain such elements down to 50 m depth (Chitea, 2016).

The ERT method has also been used in conjunction with deeper sounding methods (magnetotellurics) (Sung *et al.*, 2010). Deeper sounding electromagnetic (EM) methods were less frequently applied, as EM waves are strongly attenuated in this very conductive environment. Despite this, the use of two or more EM methods may allow to overpass the limits of each method (poor resolution at shallow depths in case of low frequency operating techniques and limited depth of investigation for high frequencies methods in such very conductive environment). The utilization of Transient Electromagnetic Method (TEM) and radiomagnetotellurics (RMT) (Adrian *et al.*, 2015; Tezkan *et al.*, 2012) proved to be useful in advancing the knowledge upon the subsoil resistivity distribution in an area affected by mud volcanism, but still the maximum depth of investigation was too shallow for reaching the source domain approximated at 10 km. By using long offset transient electromagnetic (LOTEM) method, the depth of investigation was greatly increased up to 5–6 km (Tezkan *et al.*, 2012).

There is a lack of data in the academic literature about the use of Spontaneous Potential method in mud volcanoes studies, despite the fact that good premise of its usage exists. In our approach, we applied Spontaneous Potential (SP) method to evaluate the possibility of using it for tracing the mud volcanoes feeder channels that branch from the main deep conduit. We overlapped electrical resistivity measurements on the SP profile in order to analyze the changes of this parameter versus the SP variation.

The deployment of geophysical measurements (Electrical Resistivity Tomography, Vertical Electrical Soundings and Spontaneous Potential) in the study area of Pâclele Mici mud volcanoes plateau from Berca (Buzău County) was constrained by both natural elements (very active large craters surrounded by fresh ejecta material) and by regulation policies (it is a touristic objective and a protected Natura 2000 – ROSCI0272 site). Therefore, the number of the profiles was limited and their placement was constrained.

The results presented in this paper are part of a first attempt to evaluate the mud volcanoes electrical signatures and to obtain a detailed knowledge of the internal structure down to shallow depth (< 40 m) for the Pâclele Mici mud volcanoes plateau.

2. GENERAL GEOLOGICAL SETTING

The study area – Pâclele Mici mud volcano site – is located within the axis of the *Berca-Arbănași anticline structur*e, which hosts clusters of mud volcanoes distributed over a 15 km long lineament. The four spots with important mud volcanoes occurrences are known as Fierbători, Pâclele Mari, Pâclele Mici, and Beciu. Despite their close locations, there are some notable differences between these sources in terms of extruded material patterns (Baciu *et al.*, 2007; Madeja, Mrowczyk, 2010).

In the formed mud plateau (Fig. 1) there are a multitude of vents with different morphological shapes (single cone type, cluster of cones, mud pools, "salses"/large pools, flank vents) and slightly different viscosity and composition of the ejecta material, as proved by pH and electrical conductivity measurements on samples taken from different vents of the same plateau (Fig. 1). The depositional rate is difficult to estimate, as low activity periods might alternate with intense activity intervals and, more rarely, with explosive phases (Mărunțeanu, Ioane, 2010).

The *Berca-Arbănași anticline* consists of sedimentary deposits that range in age (Melinte-Dobrinescu *et al.*, 2017) from Middle Miocene to Late Pliocene (Fig. 2), and that have been deposited within the Eastern Carpathians Inner Foredeep. The core of the fold includes Middle Miocene (Tortonian) salt breccia that diapirically pierced overlying deposits. Sarmatian age blocks embedded into the breccia (Ciocârdel, 1949;

Voicu, 1975; Baciu *et al.*, 2007) are the most conspicuous signature of that process. An oil and gas accumulation was trapped in the Upper Miocene (Meotian) sand-formations (Paraschiv, 1975), while the actual mud volcano structures develop (Ciocârdel, 1949) onto marly deposits of uppermost Miocene-lowermost Pliocene (Pontian) age.

Brustur *et al.* (2015) considered that the faulted flanks of the anticline have favored both diapiric migration of the Middle Miocene salt, and upflow of the fluids discharged through the mud volcanoes. It is also worth mentioning that in the Pâclele Mici mud volcano region, a strike-slip fault has induced a right-lateral displacement of the anticline axis (Ciocârdel, 1949).

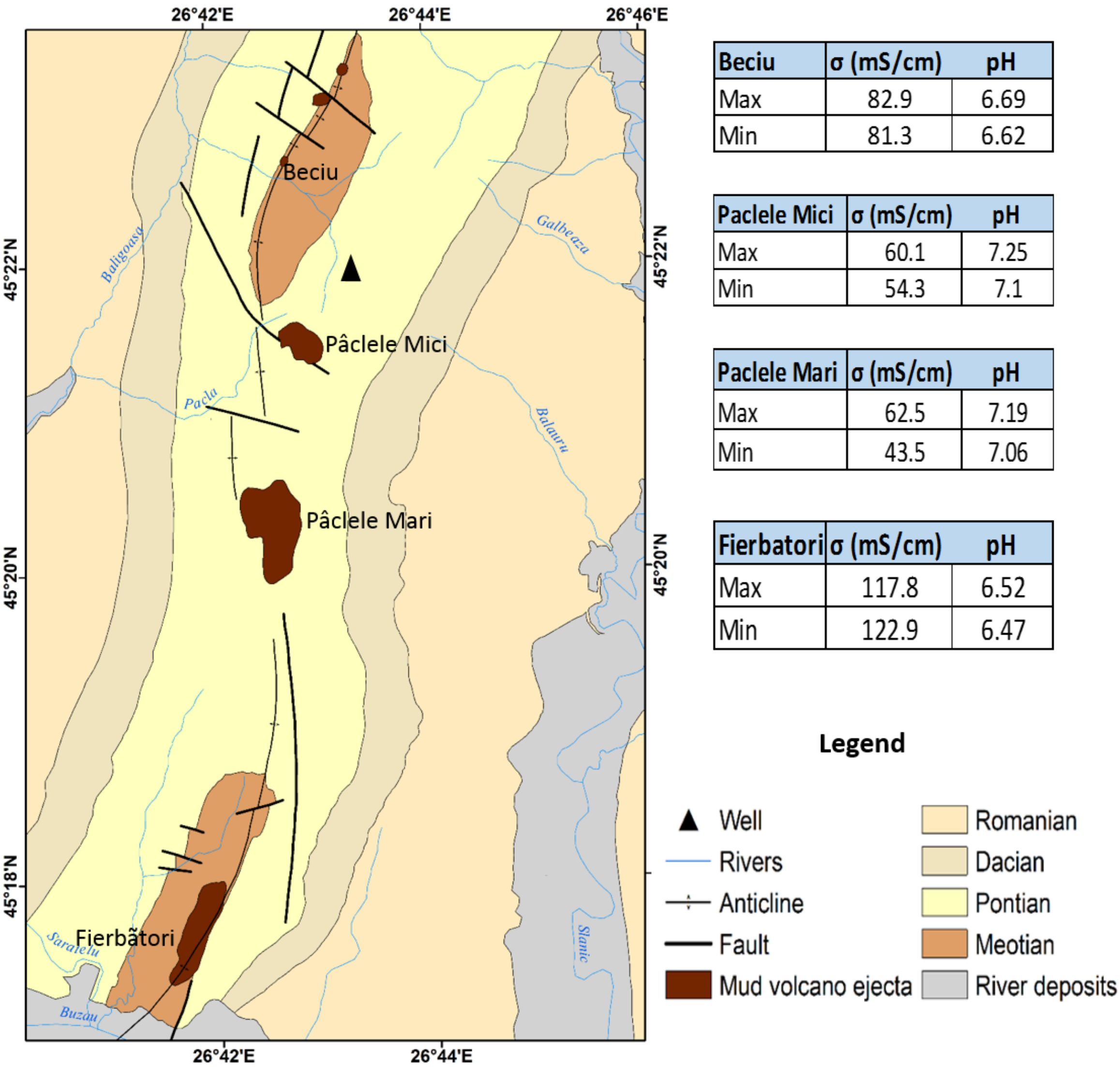

Beciu	σ (mS/cm)	pH
Max	82.9	6.69
Min	81.3	6.62

Paclele Mici	σ (mS/cm)	pH
Max	60.1	7.25
Min	54.3	7.1

Paclele Mari	σ (mS/cm)	pH
Max	62.5	7.19
Min	43.5	7.06

Fierbatori	σ (mS/cm)	pH
Max	117.8	6.52
Min	122.9	6.47

Fig. 1 – Geological map of the Berca-Arbănași anticline (after Ciocârdel, 1949, with modifications) and results of electrical conductivity (σ) and pH of mud volcano ejected liquid. The highest conductivity values were found in ejected material from the Fierbători mud volcanoes field, while the smallest content in dissolved salts was noticed for a sample collected from Pâclele Mari. The geological cross-section which intersects the marked well is given in Fig. 2.

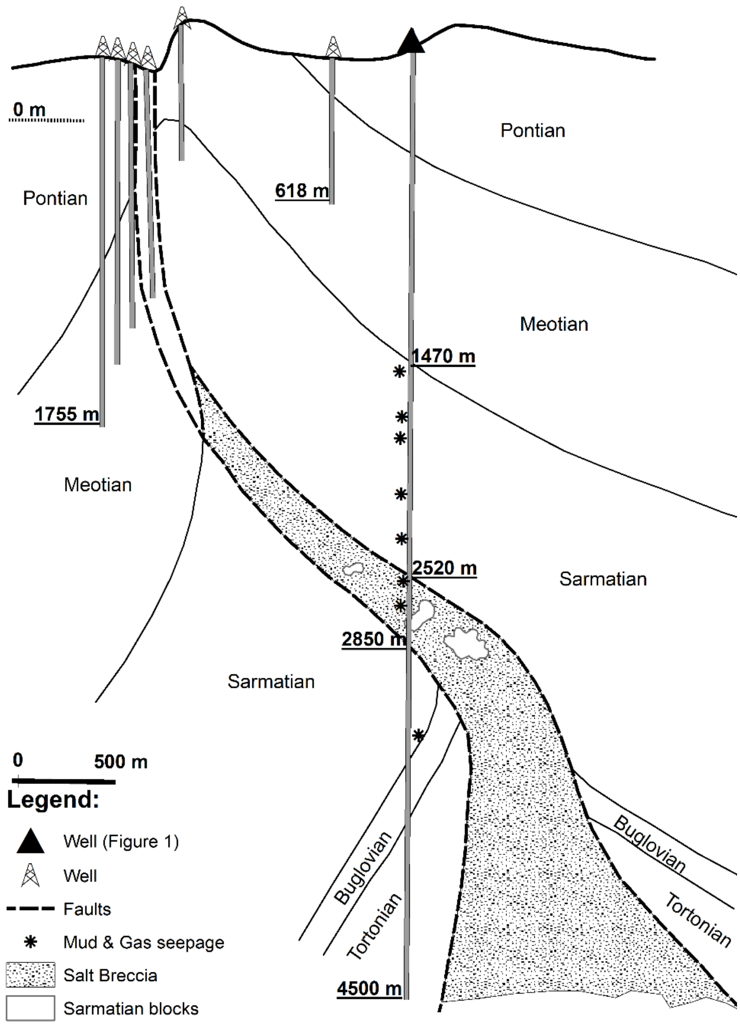

Fig. 2 – Geological cross-section (after Voicu, 1975) through the borehole with position given in Fig. 1.

3. THE EJECTED MATERIAL CHARACTERISTICS

THE GASEOUS EMISSIONS

The gas released at Pâclele Mici is methane-rich (~95% CH_4; ~2% CO_2; ~3% N_2; Baciu *et al.*, 2018), being thus quite similar to the majority of the mud volcano exhalations described worldwide (Etiope *et al.*, 2009). Isotopic analyses ($\delta^{13}C_{CH4}$ and $\delta^{2}H_{CH4}$) have proven that the Pâclele Mici gas origin was thermogenic (Etiope *et al.*, 2009). This inference is apparently contradicted by the high ratio (>1500) recorded between the methane concentration and the concentrations of the C_2-C_3 alkanes (ethane + propane), as such large ratios are often related to a microbial provenance. Baciu *et al.* (2018) assumed however that in this case, the ratio mirrored gas composition alteration induced ensuing to molecular fractionation (loss of ethane and propane) which intervened, in contact with water or mud, during the gas ascension toward the ground surface.

CHEMISTRY OF THE GROUNDWATER EXPELLED BY THE MUD-VOLCANOES

For the Pâclele Mici brine, two chemical analyses are available: one published by Sencu (1985), and the other one by Madeja, Mrowczyk

(2010). A remarkable chemical facies similarity is visible for these groundwater samples (Fig. 3) that have been collected at 25–30 years time-interval.

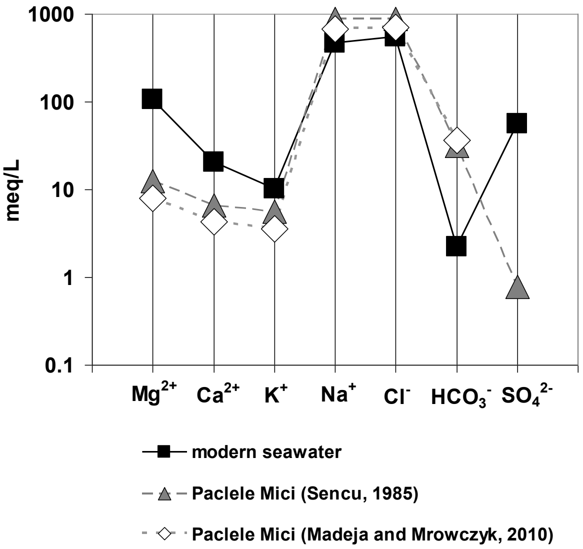

Fig. 3 – Schoeller diagram of the saline groundwater samples collected from the mud volcanoes site.

Based on these results several distinctive features are noticed:

(i) The mud volcano brine concentrations of Na^+ and Cl^- (expressed as meq/L) are virtually equal to each other (Fig. 3) – a circumstance that rather suggests a halite leaching origin (see, in this respect, also the Na^+ vs. Cl^- concentration plot – Fig. 4 – in which the analyzed samples data-points fall on the halite dissolution line, rather than on the line corresponding to modern seawater dilution/evaporation);

(ii) Although the brines' contents of Na^+ and Cl^- are of the same order of magnitude as the corresponding seawater concentrations (Fig. 3), the constituents SO_4^{2-}, Mg^{2+}, and Ca^{2+} exhibit – with respect to modern seawater contents – strong depletions;

(iii) The Br- vs. Cl- plot (Fig. 5) indicates for the Pâclele Mici brine a Cl-/Br- mass ratio of 678. It is usually interpreted (*e.g.*, Martin, 1999; He *et al.*, 1999; Chen *et al.*, 2013; Stober, Bucher, 2015) that such large Cl-/Br- ratios likely correspond to a halite dissolution process: this inference relies on the observation that when seawater evaporation progresses, until halite begins to precipitate, the halite crystals will incorporate only small amounts of the Br- which was originally present in the marine liquid; therefore, brines resulted ensuing to the subsequent dissolution of the precipitated halite are depleted in Br- (hence, the Cl-/Br- ratio is larger than the corresponding seawater ratio, of 288).

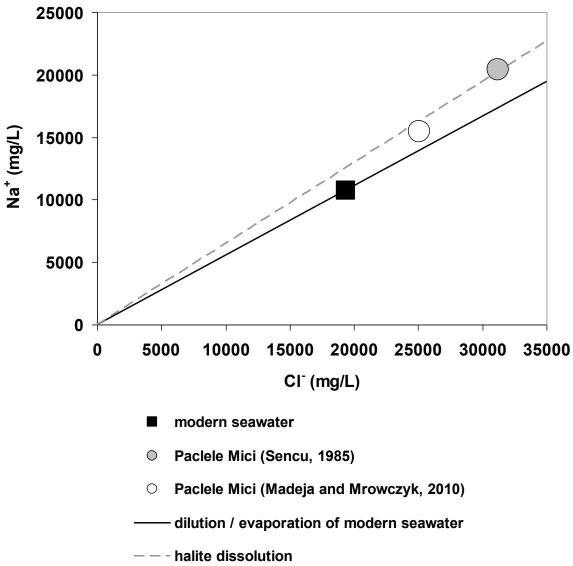

Fig. 4 – Na^+ vs. Cl^- reciprocal concentration plot constructed for the saline groundwater samples collected from the mud volcanoes site.

The origin of the expelled water has been sometimes associated (*e.g.*, Baciu *et al.*, 2007) with connate water accompanying the deep-seated oil accumulations trapped in the nearby Meotian deposits, combined with meteoric water (Mărunțeanu, Ioane, 2010). Connate water is expected to display chemical similarities with modern (*i.e.* present-day) seawater, whereas the mud volcanoes brine provides evidence that also suggest the presence of a water type with different characteristics than connate or meteoric water.

Based on the above-mentioned geochemical signatures (Cl^-/Br^- ratios and depletion in SO_4^{2-}, Mg^{2+}, Ca^{2+}), we assume that the ejected mud volcano liquid can be a mixture between different types of waters, with the strongest chemical signature being imposed by the halite-leaching brine.

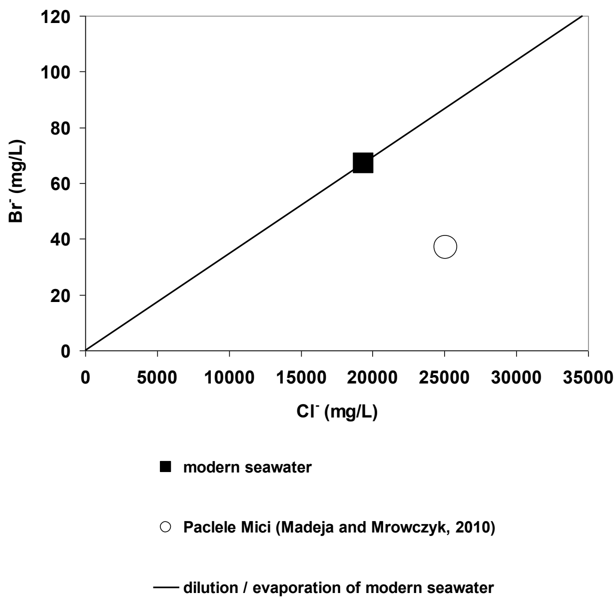

Fig. 5 – Br^- vs. Cl^- reciprocal concentration plot constructed for the saline groundwater sample collected (Madeja, Mrowczyk, 2010) from the mud volcanoes site.

The influence of meteoric water is anticipated due to on site observations, which associate higher rates of the ejecta material with an intensified rainfall regime. The influence of the meteoric water low mineralization can also explain the electrical conductivity fluctuation of the mud ejecta liquid (Fig. 1). While the expelled liquid electrical conductivity measured on samples taken in different seasons ranged between 54–60 mS/m, the closest drinking water source (positioned at ~100 m – eastern side of the mud plateau) displayed a value of only 1.12 mS/m.

CHARACTERISTICS OF THE EXPELLED SOLID PHASE

Mud volcanic products include mostly (50–60%) a fine-grained fraction (less than 0.001 mm), with millimetric clayey fragments or aggregates embedded within it (Schniukov *et al.*, 2009). In addition, limestone fragments are present, some of them having undergone a pyritisation process. Within the overall clayey matrix, veins of calcite with fluid inclusions occur, mirroring additional neoformation processes associated to the mud volcanoes activity. It was conjectured that a hydrothermal environment of low temperature (70°C at most, but likely smaller than 40°C) was responsible for the formation of those carbonate veins. Within the calcite, remarkably large concentrations of boron (0.06 – 0.2 %) have been detected.

Other detrital fragments consist of sandstones and conglomerates, from the latter deriving also, most likely, the scarcely encountered fragments of Precambrian age green schists. Up to 20 cm large carbonate concretions (ankerite, dolomite) occur as well (Schniukov *et al.*, 2009). Micro-fauna studies (Voicu, 1975) indicate that the detrital fragments originate in formations of Pontian, Meotian, Sarmatian, Tortonian, Eocene, and also – probably – Oligocene ages.

4. GEOELECTRICAL MEASUREMENTS AT PÂCLELE MICI

The geophysical survey in the Pâclele Mici mud volcano plateau (Fig. 6) consisted of the deployment of three different electrical investigation techniques: Vertical Electrical Soundings (VES), Electrical Resistivity Tomography (ERT) and Spontaneous Potential (SP).

Resistivity measurements consist of injecting a quasi-DC electrical current into the ground by means of a pair of two steel electrodes and measuring the resulted potential using another pair of electrodes. The depth of the investigation depends on the length of the array and on the subsoil characteristics. In high conductivity environment, the depth of investigation is significantly reduced.

A total number of 26 VES were measured using Schlumberger array, grouped on three alignments – profiles named VES#1, VES#2 and VES#3. Each profile consisted of 7, 13 and 6 soundings respectively, with maximum current electrodes distance ranging from 60 to 100 meters.

The Electrical Resistivity Tomography (ERT) was conducted with the dipole-dipole array, using 48 electrodes with 3 meters spacing. Data acquisition utilized a multi-channel system, collecting a dataset of 609 measurements for a surface length of 141 m.

Finally, overlapping with the ERT line, a Spontaneous Potential (SP) profile with 10 meters spacing and 180 meters length was measured, immediately after finishing the ERT measurements. The ERT and SP profiles were placed within a small distance (approximately 35 meters) from the currently most active craters (marked in Fig. 6).

The VES profiles were positioned in different parts of the Pâclele Mici zone, having as objective the near surface characterization of the area fully covered by mud volcanoes ejected material.

All VES investigated areas exhibit very low apparent resistivity values (<24 Ohm*m), that are gradually increasing with depth. The constructed apparent resistivity sections (presented in Fig. 7) reveal layering of the sediments in most areas, with a very conductive layer on top. The active mud craters samples indicate a saline NaCl-type groundwater type, such characteristics explaining the very low resistivity values determinate by the indirect investigation methods for the impregnated geological formations.

At the time of the survey there were neither any active vents along the VES profiles, nor any visible morphological shapes that could be related to a past (extinct or dormant) mud volcano crater. But due to the dynamics of the area, with activation/deactivation sequences or appearance of new vents, deep buried inactive old channels are likely to exist. To evaluate this possibility along the VES investigated alignments we used inversion techniques to obtain the true resistivity distribution of the areas surveyed by VES.

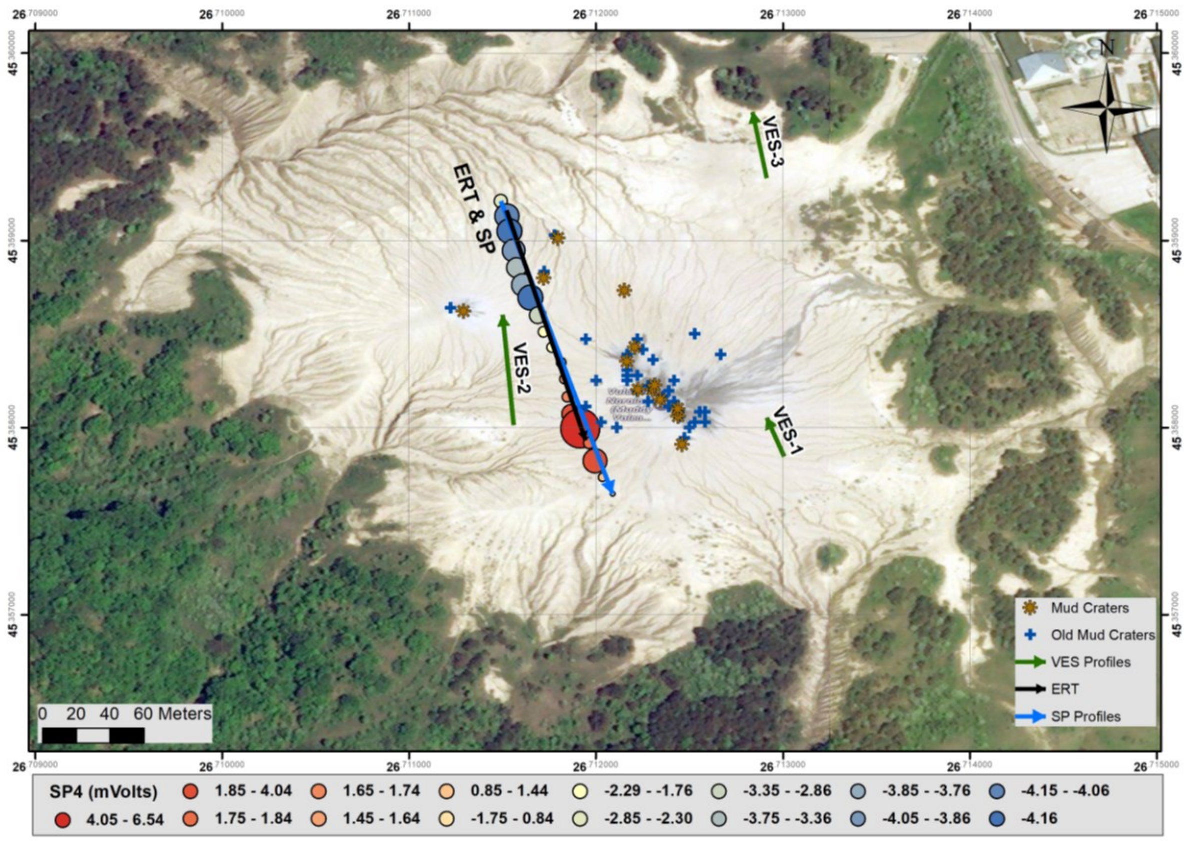

Fig. 6 – Investigated site with position of ERT-SP and VES profiles, along with results of SP measurements and active mud vents at the survey time. The “old mud craters” location is given after Brustur *et al.*, 2015.

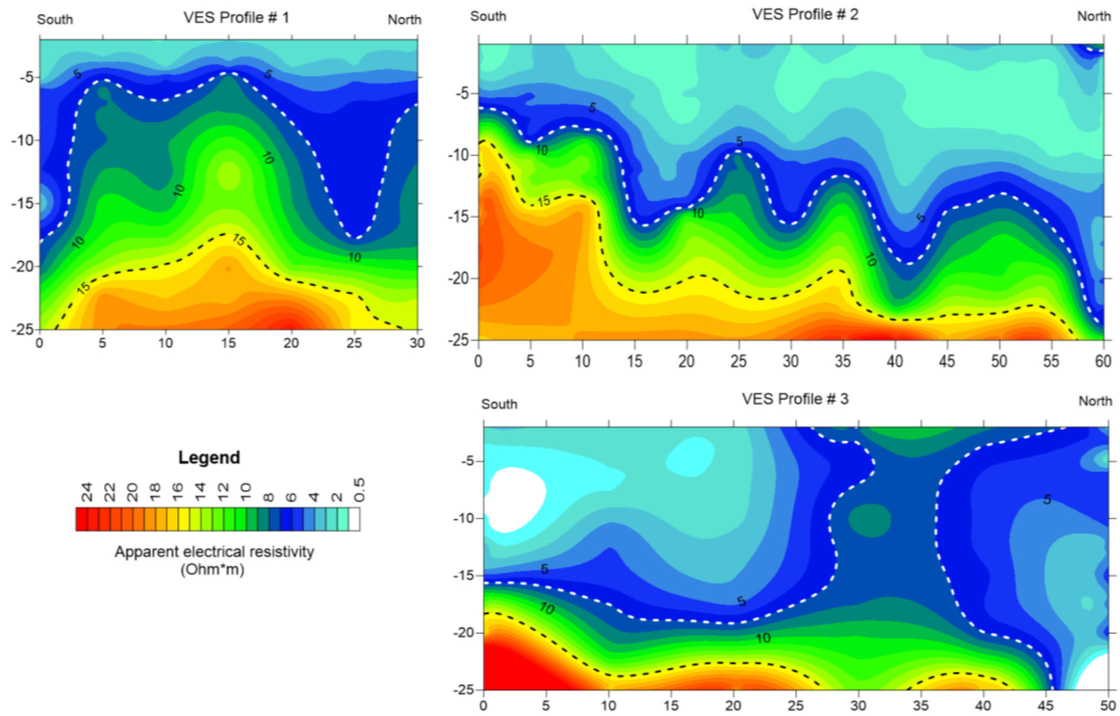

Fig. 7 – Raw electrical resistivity data represented with vertical scale expressed as AB/4
AB – the extension of the injection line used for measuring the electrical potential.

Electrical soundings were initially processed by using a 1D inversion software, which provides for each sounding independent results. The latter can be joined in order to generate a pseudo-2D model of the surveyed profile. However, due to the low contrasts between the buried sediments and the restriction of 1D interpretation in an extremely conductive geological environment, such a way of analyzing the results was considered inappropriate for this case study. Following this, a second method of inversion, based on full 2D inversion software (Kim, 2012), was used to generate inverted sections for all the VES lines. For each profile, independent collinear sounding data joined and the resulted dataset was processed by means of a customized automatic 2D inversion algorithm. The small distance (5–10 m) between successive VES stations provided a good lateral resolution. The resulted 2D inverted sections of the VES profiles #1, #2 and #3, are given in Figure 8, keeping visible only the area with adequate parameter resolution.

For comparison, all images were represented using the same color scale. VES profiles #1 and #2 reveal a gradual increase of the calculated resistivity showing a two-layered model. On VES profile #1, the first layer is very conductive (< 8 Ohm*m) and starts from the surface down to 2 meters depth. Profile VES#2, located east of the main active craters, reveals a top layer characterized by low resistivity values (approximately 2–8 Ohm*m) dominating the first 6 to 8 meters depth. In both cases the low resistivity close to the surface can be explained by the higher moisture content of these formations, either resulting from the rainwater retention or/and from the recent spill material, coming from the active vents which are placed in a higher topographic position.

The case of VES#3 is different from VES#1 and VES#2 suggesting that there is a more resistive area in the northern part and a very conductive area dominating the south part with similar characteristics as the other two profiles. For profile VES#3, the northern part of the injection line was extended out of the area that now is covered exclusively by mud volcano ejecta (in the northern, grass covered region).

Therefore, the results on the VES#3 profile, placed in the external part of the plateau, may be explained in relationship with a lateral contact between brine-saturated sediments and adjacent dryer formations.

The resulted resistivity anomalies did not outline any relatively "recent" buried feeder channels, and this result is indirectly sustained by analyses of an older database with mud volcanoes crater locations presented in Figure 6 conjointly with the active vents observed during the present geophysical survey. The comparison of the two databases of mud volcano craters revealed the continuous activity of a cluster of vents, while others spots became extinct during the ~ 7 years time-interval elapsed between the two inventories. This allowed concluding that no recent mud vents existed along the VES profiles.

In order to enhance the knowledge upon the shallow depth structure of the mud plateau, the study was continued by using the ERT technique. The ERT survey, using a multi-channel system of 48 electrodes, provided adequate resolution near the surface and allowed to reach a depth of investigation close to 40 meters. The resistivity distribution was calculated using the DC_2DPro inversion software (Kim, 2012), presented in Figure 9. The resulted model is in good accordance with the VES results, depicting a very low resistivity layer, right beneath the thin crust formed at the soil surface. The conductive layer (< 3 ohm*m) is well developed and dominates the first 10 meters below the surface indicating the presence of high moisture sediments near the surface. In the southern part of the ERT profile, the low resistivity area extends to even greater depths, suggesting that there may be a feeder channel, which discharges the salty mixture, resulting also a lateral spread of the slurry in the upper part developed right beneath a thin crust on the surface.

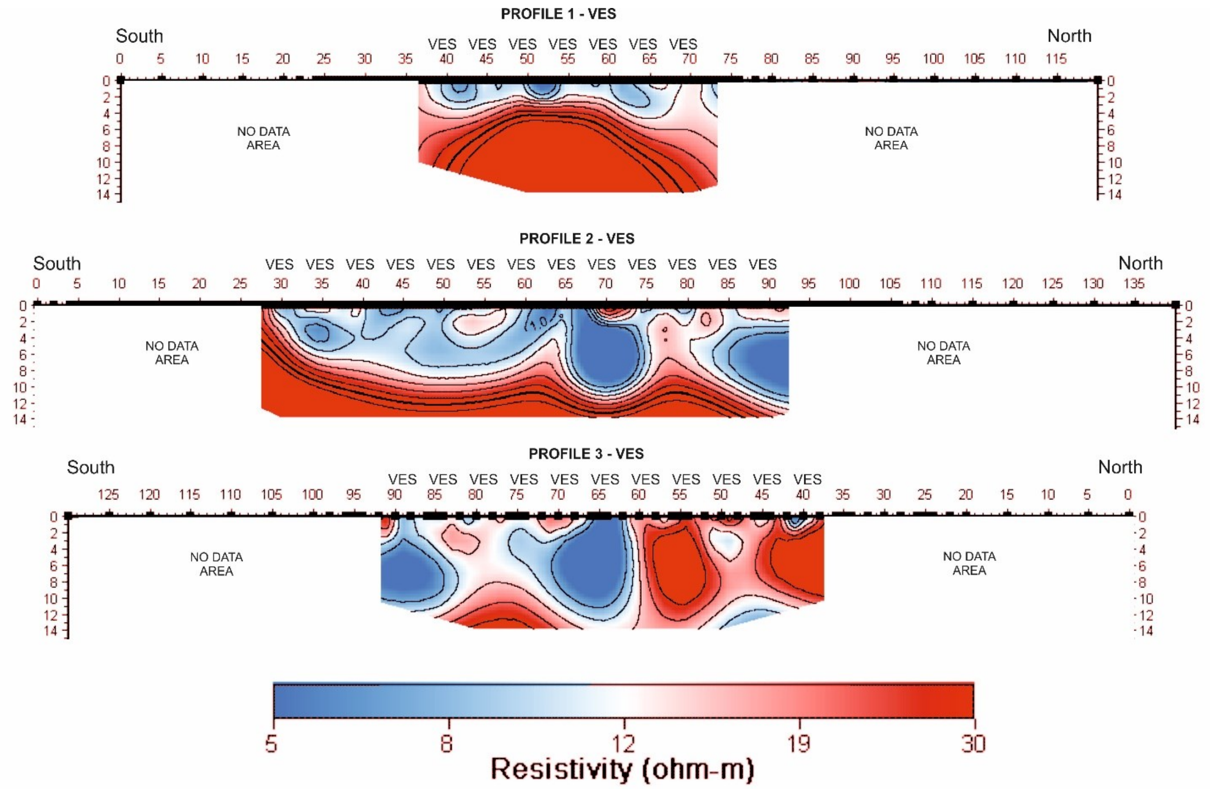

Fig. 8 – 2D inversion of VES data.

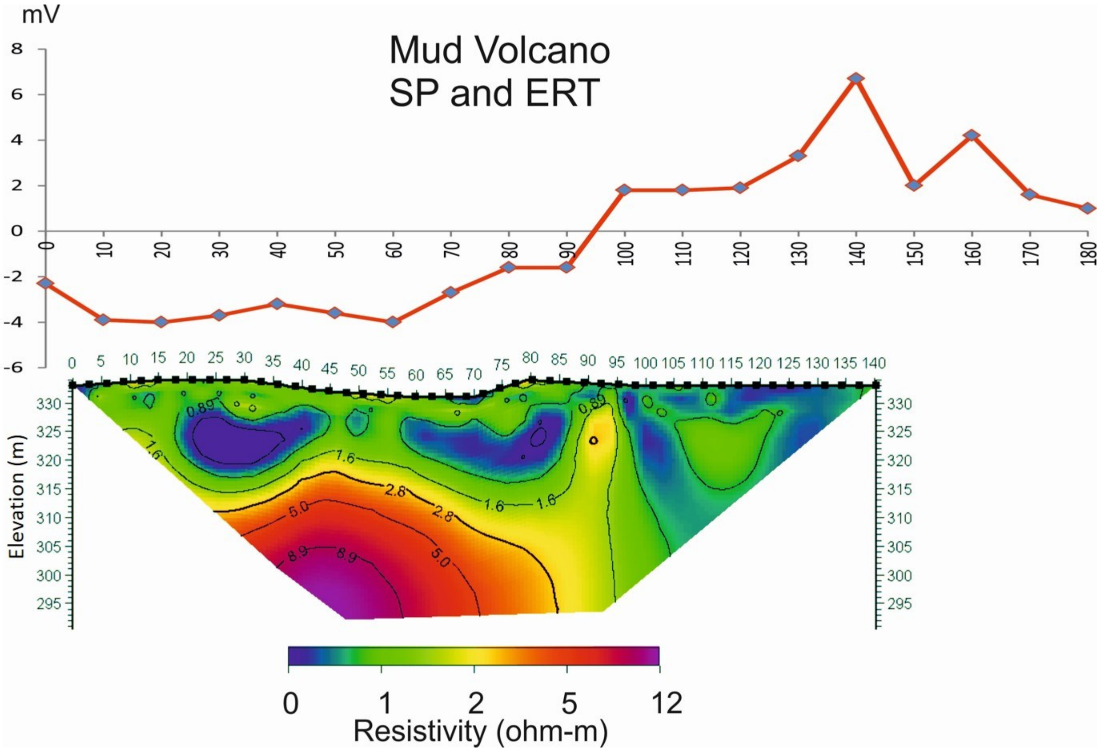

Fig. 9 – SP results and ERT inverted section.

The SP profile (180 meters long) was measured by using the "fixed reference" technique, placing one electrode as a base station in the north part of the profile, while the second electrode was moved along the survey line. Measurements were acquired in stations with 10 meters separation. The results reveal two different behaviours in the data. The first half of the profile (northern part) is dominated by negative values of few millivolts, while in the second half of the profile (southern part) the SP is increasing by more than 10 millivolts, displaying only positive values. Considering the geology of the area, the SP results were interpreted as a signature of subsurface fluid flow. As the electrolyte composition is only slightly variable (according to electrical conductivity measurements on muddy samples for different vents from this MV plateau), the variation of the voltage along the SP profile is considered to be directly related to the upward flow velocity of the muddy-fluid.

The results obtained by the two methods (ERT & SP) on the same profile are presented together for comparison (Fig. 9). A strong correlation is noticed between the very conductive southern part of the ERT survey line and the area where the SP increases before dropping again close to the end of the profile. These results are correlating well with the presence of the cluster of active vents (where the mud flows upwards) being supplied with fresh material by a deeper feeder channel. In that specific area, the number of active craters is significantly larger than the numbers of craters observed in the northern part of the surveyed area (Fig. 6).

5. DISCUSSION AND CONCLUSIONS

Resistivity measurements performed using Vertical Electrical Soundings and Electrical Resistivity Tomography acquisition techniques revealed that the subsurface is dominated by very low resistivity values that indicate the presence, in the entire considered area, of fine-grained sediments highly impregnated with saline water. The few chemical analyses available for the groundwater discharged by the Pâclele Mici mud volcanoes confirm the geophysical observations and suggest that the discharged water composition is significantly controlled by halite leaching.

The geoelectrical results also outlined that the corresponding eruption mechanism involves a lateral spread at shallow depths of the upraised fluids. This observation suggests changes in sediments permeability or an effect of significant decrease of the muddy material energy at shallow depth.

A very good correlation was observed between the SP values and the cluster of active volcanoes, showing that by means of this method, mud channels that are subject to active upflow can be traced. The SP results (higher values for the southern part of the profile) were in good agreement with the ERT vertically-extended low resistivity anomaly and with the position of active vents.

However, as observed also in this study, the electrical resistivity methods application in an area of active mud volcanoes can be restricted, as the placement of profiles in certain locations of maximum interest (such as exactly above an active mud volcano) cannot be always achieved. The crater diameter can be sometimes larger than the configured distance between electrodes, or the nearby area cannot be accessed due to conservation regulations (Mud Volcanoes from Pâclele Mici, Romania, are part of a protected site), or to safety constraints. There are several deep (some up to 2.5 m), abrupt and wide trenches in the area surrounding Pâclele Mici, caused by water erosion, this circumstance also limiting the deployment of geoelectrical profiles. In addition, due to the very low resistivity environment, the depth of investigation by geoelectrical methods (ERT and VES) is highly reduced.

The exploration of the shallow depth internal structures of mud volcanoes has made some progress by use of VES, ERT and SP data, enhancing the knowledge upon the geoelectrical data resolution and applicability in such low contrast and extremely conductive environment, opening the possibilities of further studies. Based on these results, we consider that only a joined SP & ERT survey and/or monitoring program can lead to better understanding the mud volcanoes near-surface structures, its behavior in time and the correlation of its activity with the strong seismic shocks of Vrancea area.

REFERENCES

ACCAINO, F., BRATUS, A., CONTI, S., FONTANA, D., TINIVELLA, U. (2007), *Fluid seepage in mud volcanoes of the northern Apennines: an integrated geophysical and geological study*. Journal Geophysical Research, **63**, pp. 90–101.

ADRIAN, J., LANGENBACH, H., TEZKAN, B., GURK, M., NOVRUZOV, A.G., MAMMADOV, A.L. (2015), *Exploration of the Near-surface Structure of Mud Volcanoes using Electromagnetic Techniques: A Case Study from Perekishkul, Azerbaijan.* JEEG, **20**, Issue 2, pp. 153–164, DOI: 10.2113/JEEG20.2.153

BACIU, C., CARACAUSI, C., ETIOPE, G., ITALIANO, F. (2007), *Mud volcanoes and methane seeps in Romania: main features and gas flux.* Annals of Geophysics, **50**, No. 4, pp. 501–511.

BACIU, C., IONESCU, A., ETIOPE, G. (2018), *Hydrocarbon seeps in Romania: Gas origin and release to the atmosphere.* Marine and Petroleum Geology, **89**, Part 1, pp. 130–143.

BARBER, A.J., TJOKOSAPOETRO, S., CHARLTON, T.R. (1986), *Mud volcanoes, shale diapirs, wrench faults and melanges in accretionary complexes, eastern Indonesia.* American Association of Petroleum Geologists Bulletin, **70**, pp. 1729–1741.

BRUSTUR, T., STĂNESCU, I., MACALEȚ, R., MELINTE, M. (2015), *The mud volcanoes from Berca: significant geological patrimony site of the Buzău land geopark (Romania).*

CHEN, J., LIU, D., PENG, P., YU, C., ZHANG, B., XIAO, Z. (2013), *The sources and formation processes of brines from the Lunnan Ordovician paleokarst reservoir, Tarim Basin, northwest China.* Geofluids, **13**, Issue 3, pp. 381–394.

CHITEA, F. (2016), *Electrical signatures of mud volcanoes – Case studies from Romania,* 16th International Multidisciplinary Scientific GeoConference – SGEM 2016, Conference Proceedings, Book 1, Vol. 3, pp. 467–474, ISBN 978-619-7105-57-5 /DOI: 10.5593/SGEM2016/B13/S05.059

CIOCÂRDEL, R. (1949), *Regiunea petroliferă Berca–Beciu–Arbănași. Institutul Geologic al Academiei R.P.R.* Studii Technice şi Economice, seria A, vol. **4**, 32 pp.

DIACOPOLOS, C., STOCHICI, R. (2016), *Vertical electrical sounding (VES) in areas with mud volcanoes. Case study: Muddy volcanoes of Păclele Mari, Romania.* Geoscience 2016, Abstracts volume.

DIMITROV, L.I. (2002), *Mud volcanoes – the most important pathway for degassing deeply buried sediments*. Earth-Science Reviews, **59**, pp. 49–76.

ETIOPE, G., BACIU, C., CARACAUSI, A., ITALIANO, F., COSMA, C. (2004), *Gas flux to the atmosphere from mud volcanoes in Eastern Romania.* Terra Nova, **16**, Issue 4, pp. 179–184.

ETIOPE, G., FEYZULLAYEV, A., BACIU, C.L. (2009), *Terrestrial methane seeps and mud volcanoes: a global perspective of gas origin.* Marine and Petroleum Geology, **26**, Issue 3, pp. 333–344.

HE, K., STOBER, I., BUCHER, K. (1999), *Chemical evolution of thermal waters from limestone aquifers of the Southern Upper Rhine Valley.* Applied Geochemistry, **14**, Issue 2, pp. 223–235.

HOVLAND, M., JUDD, A. (1988), *Seabed pockmarks and seepages: impact on geology, biology and the marine environment.* Graham and Trotman, London, 293 pp.

IVANOV, M.K., LIMONOV, A.F., WOODSIDE, J. (Eds.) (1992), *Geological and geophysical investigations in the Mediterranean and Black Seas.* Initial results of the "Training-through-Research" Cruise of RV Gelendzhik in the Eastern Mediterranean and the Black Sea, June–July 1991, UNESCO Reports in Marine Science, **56**, 208 pp.

JUDD, A., HOVLAND, M. (1992), *The evidence of shallow gas in marine sediments,* Continental Shelf Research, **12**, No. 10, pp. 1081–1095.

KHARAKA, Y.K., MARINER, R.H. (1989), *Chemical geothermometers and their application to formation waters from sedimentary basins.* Thermal History of Sedimentary Basins (eds. N.D. Naeser and T.H. McCulloh), Springer, New York, pp. 99–117.

KIM, J.H. (2012), DC 2DPro v. 0.99. User's Guide. http://kigam.en.ecplaza.net/

MADEJA, G., MROWCZYK, P. (2010), *Phenomenon of mud volcanoes in western Romania as a geoturism object.* Proceedings of the XIX-th Congress of the Carpatho-Balkan Geological Association, September 23–26, 2010, Thessaloniki, Greece, p. 491–502.

MARTIN, J.B. (1999), *Nonconservative behavior of Br^-/Cl^- ratios during alteration of volcaniclastic sediments.* Geochimica et Cosmochimica Acta, **63**, Issues 3–4, pp. 383–391.

MAZZINI, A. (2009), *Mud volcanism: Processes and implications.* Marine and Petroleum Geology, **26**, pp. 1677–1680.

MĂRUNȚEANU, C., IOANE, D. (2010), *Muddy volcanoes.* Natural Heritage from East to West, Springer, pp. 79–86.

MELINTE-DOBRINESCU, M.C., BRUSTUR, T., JIPA, D., MACALEȚ, R., ION, G., ION, E., POPA, A., STĂNESCU, I., BRICEAG, A. (2017), *The geological and palaeontological heritage of the Buzău Land Geopark (Carpathians, Romania).* Geoheritage, **9**, Issue 2, pp. 225–236.

OLENCHENKO, V.V., SHNYUKOVB, YE.F., GAS'KOVAC, O.L., KOKHC, S.N., SOKOLC, E.V., BORTNIKOVAA, S.B., EL'TSOVA, I.N. (2015), *Explosion Dynamics of the Andrusov Mud Vent (Bulganak Mud Volcano Area, Kerch Peninsula, Russia).* Doklady Earth Sciences, **464**, Part 1, pp. 951–955.

PARASCHIV, D. (1975), *Geologia zăcămintelor de hidrocarburi din România.* Studii tehnice şi economice, Institutul de Geologie şi Geofizică, Seria A, **10**, 363 pp.

PEREZ-GARCIA, C., BERNDT, C., KLAESCHEN, D., MIENERT, J., HAFFERT, L., DEPREITER, D., HAECKEL, M. (2011), *Linked halokinesis and mud volcanism at the Mercator mud volcano, Gulf of Cadiz.* Journal of Geophysical Research, **116**, B05101, doi:10.1029/2010JB008061

RAINONE, M.L., RUSI, S., SIGNANINI, P., TORRESE, P. (2012), *The contribution of shallow electrical and seismic imaging to the study of the hydrogeology of mud volcanoes: an example from Abruzzo.* Flowpath 2012. Percorsi di Idrogeologia, Bologna, Italy.

SCHNIUKOV, E.F., PANIN, N.S., DINU, C., KUTNIY, V.A., MASLAKOV, N.A. (2009), *Mud-volcanoes of Romania. Preliminary data on the mineralogy of Pâclele Mari and Pâclele Mici mud-volcanoes.* Geo-Eco-Marina, **15**, pp. 131–137.

SENCU, V. (1985), *Vulcanii noroioşi de la Berca.* Editura Sport-Turism, Bucureşti, 21 pp.

SUNG, Q.-C., CHANG, H.-C., LIU, H.-C., CHEN, Y.-C. (2010), *Mud volcanoes along the Chishan fault in Southwestern Taiwan: A release bend model.* Geomorphology, **118** (2010), pp. 188–198.

STOBER, I., BUCHER, K. (2015), *Hydraulic and hydrochemical properties of deep sedimentary reservoirs of the Upper Rhine Graben, Europe.* Geofluids, **15**, Issue 3, pp. 464–482.

TEZKAN, B., GROSSBACH, H., ADRIAN, J., HAROON, A., NOVRUZOV, A. (2012), *On the Exploration of Mud Volcanoes using Electromagnetic Techniques: a Case Study from Azerbaijan.* Near Surface Geoscience 2012 – 18th European Meeting of Environmental and Engineering Geophysics, Paris, France.

VOICU, G. (1975), *Micro-paleontological and geological observations concerning the Mio-Pliocene of Berca Region (Buzău).* Studii şi cercetări de geologie, geofizică, geografie, seria Geologie, **20** (1), pp. 143–150 (in Romanian).

ZEYEN, H., PESSEL, M., LEDÉSERT, B., HÉBERT, R, BARTIER, D., MIKAËL, S., LALLEMANT, S. (2011), *3D electrical resistivity imaging of the near-surface structure of mud-volcano vents.* Tectonophysics, doi:10.1016/j.tecto.2011.05.007

Received: May 24, 2018
Accepted for publication: July 2, 2018